

Hawkes process model with a time-dependent background rate and its application to high-frequency financial data

Takahiro Omi,* Yoshito Hirata, and Kazuyuki Aihara
*Institute of Industrial Science, The University of Tokyo,
 4-6-1 Komaba, Meguro-ku, Tokyo 153-8505, Japan.*

(Dated:)

A Hawkes process model with a time-varying background rate is developed for analyzing the high-frequency financial data. In our model, the logarithm of the background rate is modeled by a linear model with variable-width basis functions, and the parameters are estimated by a Bayesian method. We find that the data are explained significantly better by our model as compared to the Hawkes model with a stationary background rate, which is commonly used in the field of quantitative finance. Our model can capture not only the slow time-variation, such as in the intraday seasonality, but also the rapid one, which follows a macroeconomic news announcement. We also demonstrate that the level of the endogeneity of markets, quantified by the branching ratio of the Hawkes process, is overestimated if the time-variation is not considered.

PACS numbers: 89.65.Gh, 05.45.Tp, 05.40.-a, 89.75.-k

I. INTRODUCTION

In a variety of complex systems, the activity is driven by endogenous (internal) and exogenous (external) forces, exhibiting complex dynamics. Such dynamics can be observed from natural science to social science, and the examples include earthquakes [1–5], neuronal firing [6–8], human activity [9, 10], and financial market activity [11, 12]. Identifying whether the endogenous force, the exogenous force, or an interplay between the two is a major cause of the observed dynamics is important for the understanding of the system. In the context of economics, a question of what causes movements in financial markets has been a central problem for a long time. A classical paradigm of the efficient market hypothesis indicates that the market movements are fully governed by the arrival of news, that is, exclusively of exogenous origin [11]. On the other hand, the empirical evidence has been accumulated that the news arrivals can explain only a part of the large movements, and that the market activity is thus largely of endogenous origin [13, 14]. The endogenous effect of the markets is referred to as the reflexivity in the field of finance [12]. To quantify the relative importance of each factor, appropriate modeling of the observed activity is necessary.

Filimonov and Sornette (2012) [15] proposed to model the high-frequency financial data with a Hawkes process for quantifying the level of the reflexivity of the market. The Hawkes process is a simple self-exciting point process to describe temporal clusters of events [16]. In our situation, each event corresponds to a market movement. In the Hawkes process, it is assumed that every event can trigger new events, and their occurrence rate is a sum of the background rate (exogenous effect) and the triggering effect from the preceding events (endogenous effect). The strength of the endogeneity of the process is quantified by the average number of events that a single

event directly triggers (the branching ratio). By using the Hawkes model, it has been shown that a significant fraction of the market movements on the S&P E-mini futures contracts is of endogenous origin [15, 17]. In this way, the Hawkes process modeling is useful in analyzing the high-frequency financial data, and have become much popular in the domain of quantitative finance in this decade [18–20] (also see references in [21]).

In the most studies of the Hawkes process in finance, the background rate in the model is assumed to be constant in time. However this assumption is not reasonable because the trading activity is non-stationary in general. For example, it is well known that there is an intra-day seasonality, called U-shape pattern, where the activity is high around the opening and the closing of the session [15, 22]. In addition, an announcement of macroeconomic news, especially with surprising information, temporarily enhances the market activity [23], and it has been recently shown that the activity in a foreign exchange market after the macroeconomic news can be better described by a Hawkes model with a time-dependent background rate that exponentially decreases in time from the announcement [24]. Therefore it is necessary to consider the non-stationarity in the background rate to appropriately model the market dynamics.

In this paper, we assume that the background rate varies in time, and develop an estimation method. We demonstrate the effectiveness of our model by applying it to the synthetic data and the actual high-frequency data of Nikkei 225 mini futures contracts. We also examine the impact of the non-stationarity on the estimate of the branching ratio. We finally estimate the branching ratio of the market movements in Nikkei 225 mini.

II. THE DATA

We use the tick data of Nikkei 225 mini, a futures contract on the value of the Nikkei stock average, purchased from the JPX data cloud (<http://db-ec.jpx.co.jp/>).

* omi@sat.t.u-tokyo.ac.jp

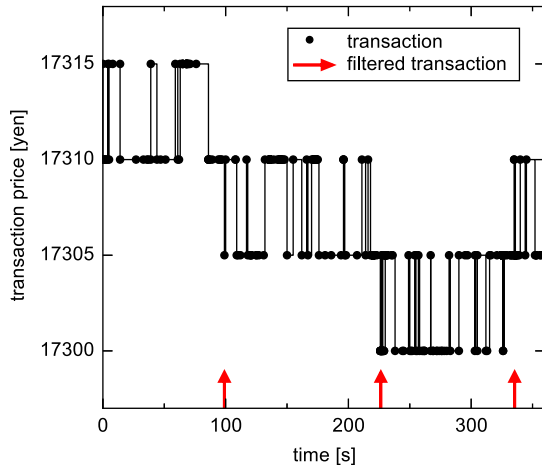


FIG. 1. Example of the transaction price change (black dots) and the filtered transactions (red arrows; see text for the detail). The time series of the filtered transactions is analyzed in this study.

Specifically, we analyze the data in the regular session (9:00-15:10 JST) from January 4, 2016 to June 30, 2016. The dataset includes the time stamps, the volumes, and the prices of all the transactions. The time stamps are recorded with a resolution of 1 second, and multiple events within the same interval of 1 second have the same time stamp. To avoid the estimation bias from the rounding procedure, we add a uniform random number $[-0.5, 0.5(\text{seconds})]$ to each time stamp. The tick size of the transaction price is 5 yen. Nikkei 225 mini deals with the 16 contracts with different expiry dates. For each session, we only use the most actively traded contract among them, the trade volume of which is 91% of the total volume on average.

The change in the transaction price is not a good indicator of a market movement because the transaction price is subject to "microstructure" noise; the transaction price rapidly jumps back and forth between the best bid and ask prices in a liquid market (the bid-ask bounce; see Fig. 1) even if the best bid and ask prices remain the same. Therefore, the change of the mid price, that is, the average of the best bid and ask prices, has been commonly used instead as a better indicator of the market movement [15, 17]. However, our dataset does not include the information on the bid and ask prices. Thus we alternatively filter the transactions for denoising the data in a following way (Fig. 1). We first exclude the transactions without the price change from the dataset. We then select the transactions satisfying the condition that (i) the sign of the price change is the same as its previous transaction or (ii) the magnitude of the price change is greater than one tick size. The filtered transactions account for about 3% of all the transactions, and the average number per session is 2090 on average, ranging from 465 to 18505. In this study, we regard the filtered transaction as the market movement, and analyze the time series of the filtered transactions.

III. MODEL

A Hawkes process is a simple point process model to describe the clustering behavior of event occurrences [16]. The original model and the extended models have been used in many fields [25–28]. In the Hawkes process, the occurrence rate $\lambda(t)$ of events at time t conditional on the occurrence history H_t is given as

$$\lambda(t|H_t) = \mu(t) + \sum_{t_i < t} g(t - t_i), \quad (1)$$

where the first term $\mu(t)$ is a background rate, and the second term represents the triggering effect from the preceding events at the occurrence times t_i , the strength of which is controlled by a memory kernel function $g(\cdot)$. We use an exponential function for the memory kernel function throughout this study,

$$g(s) = \alpha \beta e^{-\beta s}, \quad (2)$$

where α and β are parameters. In this parameterization, the parameter α corresponds to the branching ratio, that is, the average number of events that are directly triggered by a single event: $\int_0^\infty g(s)ds = \alpha$. The branching ratio is also interpreted as a ratio of the events of endogenous origin to all the events.

In most studies so far, it is assumed that the background rate is constant in time, $\mu(t) = \mu_c$ (but see [35]). In this case, the model is characterized by the three parameters $\theta = \{\mu_c, \alpha, \beta\}$, and they can be estimated by a maximum likelihood method [29]. The log-likelihood function of the Hawkes process of given parameters θ based on the data $\mathbf{D}^{[S,T]} = \{t_i\}_{i=1}^n$ of n events in an observation interval $[S, T]$ is given as

$$\log L(\theta|\mathbf{D}^{[S,T]}) = \sum_{i=1}^n \log \lambda(t_i|H_{t_i}) - \int_S^T \lambda(t|H_t)dt. \quad (3)$$

We here develop a model where the background rate $\mu(t)$ varies in time. In this section, we only briefly summarize the method, and the details are described in Appendix. In this study, $\log \mu(t)$ is modeled by a linear regression model with m given basis functions $\{f^j(t)\}_{j=1}^m$ and parameters $\{a_j\}_{j=1}^m$ as follows:

$$\log \mu(t) = \sum_{j=1}^m a_j f^j(t). \quad (4)$$

The linear model is considered for $\log \mu(t)$ since $\mu(t)$ only takes positive values. The basis functions $\{f^j(t)\}_{j=1}^m$ are bump shaped based on the cubic B-spline base $f(\cdot)$, which is a smoothly connected piecewise cubic function as shown in Fig. 2a, and their width are variable according to the frequency of the events: the width is small (large) for the high (low) frequency region (Fig. 2c). These variable-width basis functions are constructed by transforming fixed width spline bases placed in the time coordinate (natural time) where the events are evenly

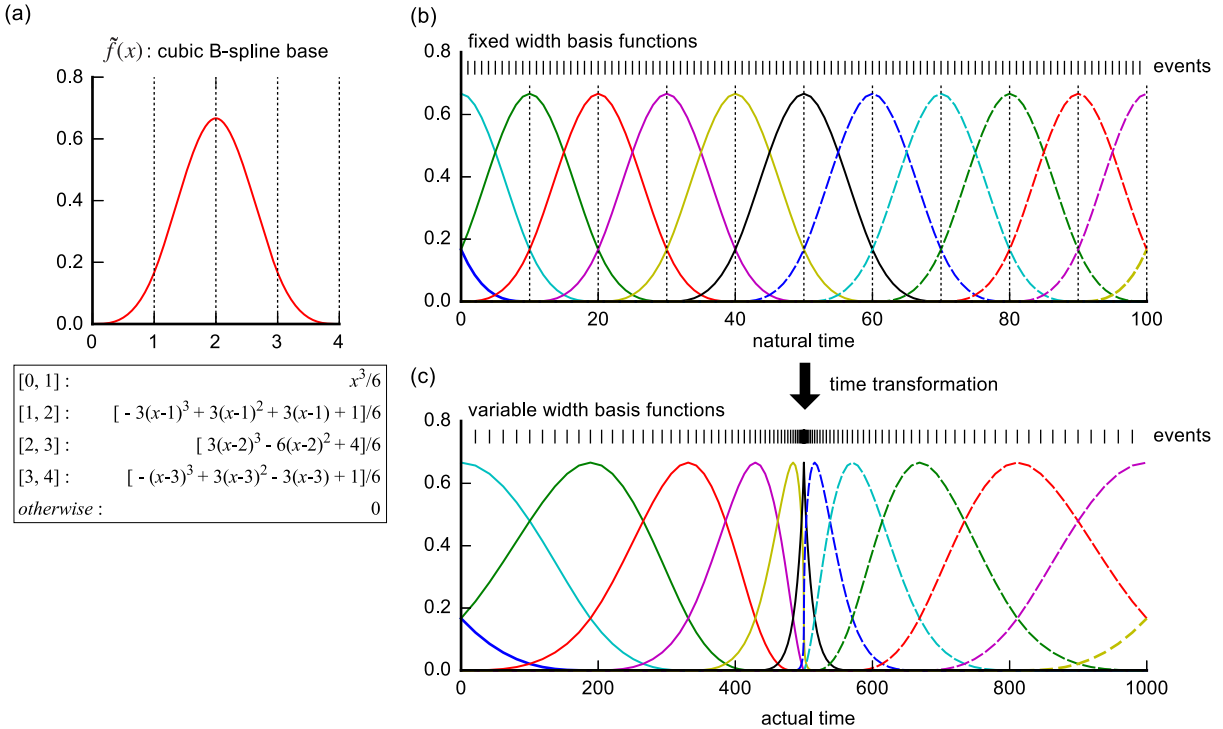


FIG. 2. Schematic view of generating the variable-width basis functions. See Appendix A for the detail method. (a) A cubic B-spline base. (b) We first place the events in an equidistant manner, and put the cubic B-spline bases with equal width. This time-coordinate is called natural time. (c) We then make a coordinate change from the natural time to the actual time to obtain basis functions with variable width.

spaced (Fig. 2b and c; see Appendix A for the detail). Such basis functions give us a flexible estimation even from the data of highly non-uniformly distributed events, as shown later. The number of the basis functions m is set to $3 + \lfloor n/100 \rfloor$, where $\lfloor \cdot \rfloor$ represents the nearest integer function. The results obtained below remain the same qualitatively against the variation of the number of the basis functions: actually we have checked the cases of $m = 3 + \lfloor n/50 \rfloor$ and $3 + \lfloor n/200 \rfloor$. In our model, the number of the parameters of the basis functions $\{a_j\}_{j=1}^m$ is large for some data (e.g., the order of hundreds). In such a case, the maximum likelihood estimation gives the rough estimates of $\mu(t)$ due to overfitting and tends to be computationally unstable. To obtain a reliable estimation, we here employ a Bayesian framework with a smoothness constraint for $\mu(t)$ (see Appendix B for the detail of the estimation procedure). The Bayesian method has been commonly employed to estimate the time-varying parameter from point process data [30–32]. In the following, we call our new model the non-stationary Hawkes model, and call the original model the stationary Hawkes model for simplicity.

To demonstrate the performance of our model, our model was applied to synthetic data simulated from the Hawkes process with a given time-varying background rate $\mu(t)$ (Fig. 3). The first example of $\mu(t)$ mimics the U-shape of the intraday pattern (Fig. 3a). We found that the estimates by our model well agreed with the true values of $\mu(t)$, α , and β . In the second example,

we considered the discontinuous rise and following decay of the background activity, which mimics the market behavior after an announcement of important macroeconomic news (Fig. 3b) [24]. Since $\mu(t)$ is modeled by a smooth function, our model cannot exactly reproduce such discontinuous behavior. Actually, a close inspection of Fig. 3b shows that the estimated $\mu(t)$ started to increase just before the true rise. However, despite such a disadvantage, our method reasonably captured the trend of the true $\mu(t)$ owing to the use of the variable-width basis functions, and the bias in the estimate of α was slight. These results show the effectiveness of our model.

IV. RESULTS

We fitted the non-stationary Hawkes model to the data of Nikkei 225 mini in the regular session of 6 hours and 10 minutes on each business day, and obtained the separate estimates over the total of 122 days. Figure 4 shows the two contrasting examples of the estimate of background rate $\mu(t)$ associated with the dynamics of the price and the cumulative number of the market movements (the filtered transactions). In the first example (Fig. 4a), the price was almost flat, and the background rate fluctuated around a baseline except around the opening. In the second example (Fig. 4b), a sharp decline in the price was present because Bank of Japan announced to keep monetary policy unchanged and disappointed the

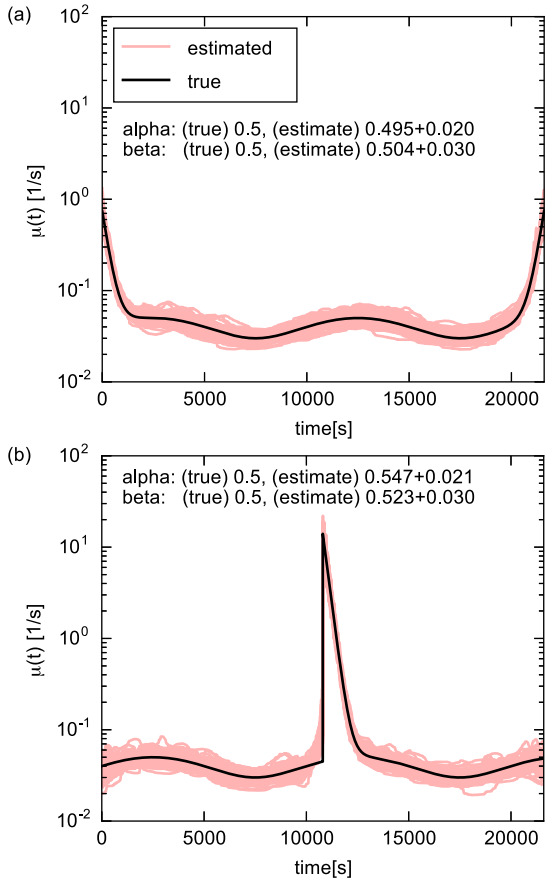


FIG. 3. Simulation study. 100 synthetic sequences are simulated by using the Hawkes process with a given background rate $\mu(t)$ (black curve). Each red curve represents the estimate of the background rate obtained by applying the non-stationary Hawkes model to each sequence. Two different background rate functions are considered in (a) and (b).

market. The decline was accompanied with the burst of the market movements and the sudden rise and decay of the background rate, which is consistent with the results in Rambaldi et al (2015). It is interesting to observe that the form of the decay was not so simple: the background rate increased again about 30 minutes after the announcement.

To examine the intraday pattern in the background rate, we show the median, 50%, and 90% ranges of the background rate at each time over the whole period under consideration (Fig. 5). The background rate was clearly high around the opening of the session, especially for the first 30 minutes, but there was no clear increase around the closing of the session. This tendency was also observed for the occurrence rate of the market movements, and that of all the transactions including the ones without price change. Thus the market movement in Nikkei 225 mini exhibited the reverse J-shaped intraday pattern rather than the U-shaped pattern. We also found that there was considerable day-to-day variability in the background rate. Therefore, it is necessary to model the background rate in an adaptive way as in our model.

We quantified the degree of the improvement achieved by the non-stationary Hawkes model against the stationary Hawkes model. For this purpose, we used the goodness-of-fit scores based on the Akaike information criterion [40] and the Akaike Bayesian information criterion [42]. The score of each model takes the form $S = \arg \max \log(Likelihood) - (Penalty)$, where the penalty depends on the model complexity (see Appendix C for the detail). The improvement was measured by the difference between the scores (the larger value indicates more improvement). Figure 6a demonstrates that the fitting was significantly improved by introducing the non-stationarity of the background rate; for example, the score difference was more than 10 for the 96.7% cases. The score difference of 10 means that the non-stationary model is about 20000 times more probable than the stationary model according the data.

We also examined how the improvement depends on the range of the price variation in each session. As seen in Fig. 4a, the background rate did not vary so much for sessions with the low price variation, therefore one may expect that the improvement by our model is not so significant for such sessions as a result. The same analysis was done respectively for the low-price-variation sessions where the range of the price, the difference between maximum and the minimum price during the session, is equal to or less than its 25% quantile (220 yen) and for the high-price-variation sessions with the range equal to or greater than its 75% quantile (385 yen). We found that the improvement was significant even for the low-price-variation sessions, although the improvement was larger for the high-price-variation sessions (Fig. 6a). This improvement indicates that the temporal variation of the background rate is a general feature of the market dynamics.

We then examined the impact of the non-stationarity of the background rate on the estimate of the branching ratio, the α parameter in the Hawkes process. Figure 6b compares the estimates of the α parameter between the two models, showing that the estimated value was, on average, two times larger for the stationary model than for the non-stationary model. This gap is because, if the temporal increase of the background rate causes a burst of the events, the stationary model tries to explain the burst as a consequence of the self-excitation. As a result, if the temporal variation of the background is present, the stationary model overestimates the branching ratio, which may lead to the wrong conclusion. This overestimation can happen even in analyzing the data of a short period. For example, the branching ratio estimated from the data of the 20 minutes period including 5910 market movements indicated by a red shaded zone in Fig. 4b was 0.93 (0.46) for the stationary (non-stationary) model. In contrast to the stationary model, our non-stationary model can estimate the branching ratio more accurately by appropriately capturing the temporal variation of the background rate, which can be sometimes present even in a fine time scale.

The branching ratio estimated from the non-stationary

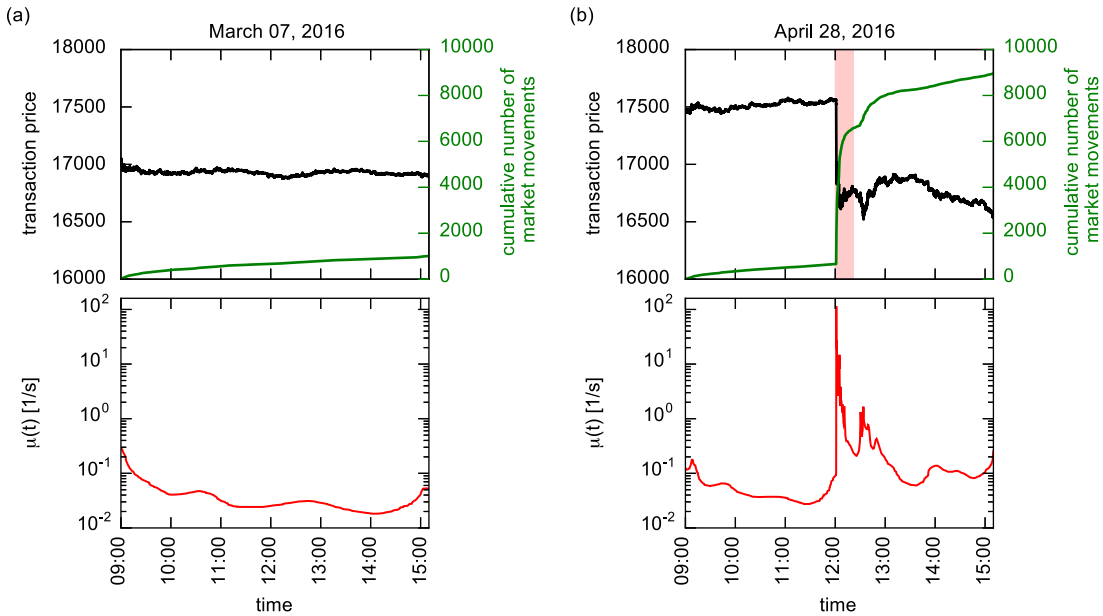


FIG. 4. Examples of the estimation of the background rate from the data of the Nikkei 225 mini for the sessions on (a) March 07, 2016 and (b) April 28, 2016. The data in a red shaded zone in (b) are re-analyzed in the later part in the section IV.

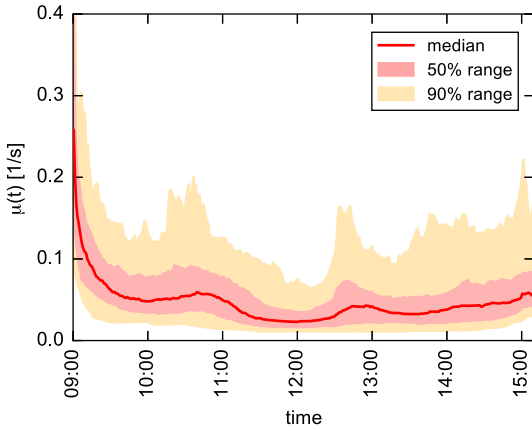


FIG. 5. The day-to-day distribution of the background rate from January 04, 2016 to June 30, 2016.

model was narrowly distributed around 0.29 (Fig. 6b), indicating that 29% of the market movements was of endogenous origin in Nikkei 225 mini. This low value means that the market activity in Nikkei 225 mini was mainly driven by the exogenous force.

V. CONCLUSION AND DISCUSSION

In this paper, we have developed the Hawkes model with a time-dependent background rate, and applied it to

the high-frequency financial data. We have demonstrated that the goodness-of-fit to the data was significantly improved by our model against the Hawkes model with a stationary background rate. We have also found the branching ratio was overestimated if the non-stationarity is not considered.

Although it has been argued that the background rate is not constant in time [15, 17, 33, 34], there has been no studies that appropriately considered the time-variation in this context, as far as we know. Therefore, a common task is to apply the Hawkes process to the data of a short period such as a few tens minutes or hours, in which the parameters may be assumed to be constant. It is noted that Lallouache and Challet (2016) modeled the temporal variation by using the piecewise linear function where the knots are placed at the intervals of 3-5 hours [35]. However, we have found that the temporal variation was sometimes present even in a fine time scale, and therefore the previous approaches may bias the results. Our model can automatically capture not only the slow variation of the intraday pattern but also the rapid variation which is observed, for example, after the announcement of the macroeconomic news, leading to more accurate estimation of the branching ratio. It is also noteworthy to mention that some models of a self-exciting point process with a non-stationary background rate have been proposed in other contexts [26, 36]. Thus the contribution of this work is the first application of the non-stationary Hawkes model to the high-frequency financial data.

[1] F. Omori, The Journal of the College of Science, Imperial University of Tokyo, Japan **7**, 111 (1894).

[2] B. Isacks, J. Oliver, and L. R. Sykes, J. Geophys. Res.

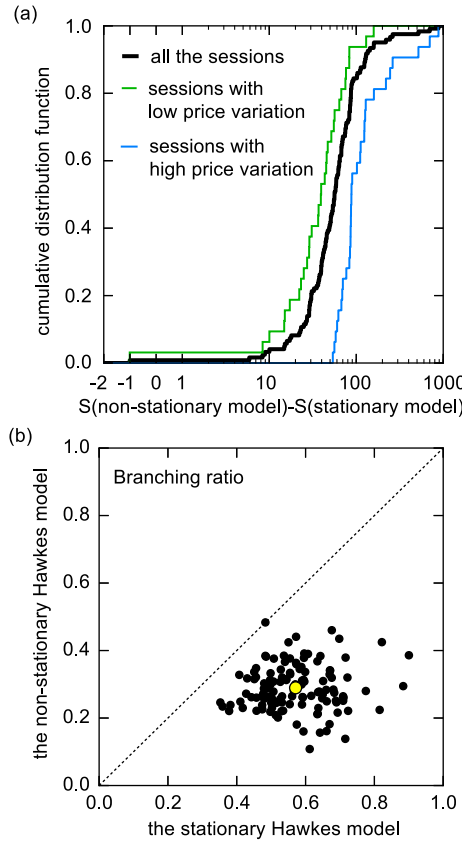


FIG. 6. The comparison between the stationary and non-stationary Hawkes models. (a) The cumulative distribution of the difference in the scores of the goodness-of-fit to the data between the two models. The black, green, and blue lines respectively represent the distribution for all the sessions, the sessions with low price variation, and the sessions with high price variation. (b) A scatter plot of the estimated branching ratio (the α parameter) between the two models. The black dot represents the estimate from the data in each trading day, and the yellow circle represents the average value.

73, 5855 (1968).

- [3] J. K. Gardner and L. Knopoff, Bull. Seismol. Soc. Am. **64**, 1363 (1974).
- [4] J. Zhuang, Y. Ogata, and D. Vere-Jones, J. Am. Stat. Assoc. **97**, 369 (2002).
- [5] D. Marsan and O. Lengliné, Science **319**, 1076 (2008).
- [6] W. Truccolo, U. T. Eden, M. R. Fellows, J. P. Donoghue, and E. N. Brown, J. Neurophysiol. **93**, 1074 (2005).
- [7] J. W. Pillow, J. Shlens, L. Paninski, A. Sher, A. M. Litke, E. J. Chichilnisky, and E. P. Simoncelli, Nature **454**, 995 (2008).
- [8] M. London, A. Roth, L. Beeren, M. Häusser, and P. E. Latham, Nature **466**, 123 (2010).
- [9] D. Sornette, F. Deschâtres, T. Gilbert, and Y. Ageon, Phys. Rev. Lett. **93**, 228701 (2004).
- [10] A.-L. Barabási, Nature **435**, 207 (2005).
- [11] E. F. Fama, J. Financ. **25**, 38 (1970).
- [12] G. Soros, *The Alchemy of Finance: Reading the Mind of the Market* (Wiley, New York, 1987).
- [13] D. M. Cutler, J. M. Poterba, and L. H. Summers, J. Portfolio Management **15**, 4 (1989).
- [14] A. Joulin, A. Lefevre, D. Grunberg, and J.-P. Bouchaud,

arXiv:0803.1769 (2008).

- [15] V. Filimonov and D. Sornette, Phys. Rev. E **85**, 056108 (2012).
- [16] A. G. Hawkes, Biometrika **58**, 83 (1971).
- [17] S. J. Hardiman, N. Bercot, and J.-P. Bouchaud, Eur. Phys. J. B **86**, 442 (2013).
- [18] P. Embrechts, T. Liniger, and L. Lin, J. Applied Probability **48**, 367 (2011).
- [19] E. Bacry, S. Delattre, M. Hoffmann, and J. F. Muzy, Quant. Finance **13** (2013).
- [20] Y. Aït-Sahalia, J. Cacho-Díaz, R. J. A. Laeven, J. Financial Economics **117**, 585 (2015).
- [21] E. Bacry, I. Mastromatteo, and J.-F. Muzy, Market Microstructure and Liquidity **1**, 1550005 (2015).
- [22] P. C. Jain and G.-H. Joh, J. Financial and Quantitative Analysis, **23**, 269 (1988).
- [23] A. M. Petersen, F. Wang, S. Havlin, and H. E. Stanley, Phys. Rev. E **81**, 066121 (2010).
- [24] M. Rambaldi, P. Pennesi, and F. Lillo, Phys. Rev. E **91**, 012819 (2015).
- [25] Y. Ogata, J. Am. Stat. Assoc. **83**, 9 (1988).
- [26] G. O. Mohler, M. B. Short, P. J. Brantingham, F. P. Schoenberg, and G. E. Tita, J. Am. Stat. Assoc. **106**, 100 (2011).
- [27] N. Masuda, T. Takaguchi, N. Sato, and K. Yano, in *Temporal Networks*, edited by P. Holme and J. Saramäki, (Springer-Verlag, Berlin, 2013), p. 245.
- [28] P. Reynaud-Bouret, V. Rivoirard, and C. Tuleau-Malot, 2013 IEEE Global Conference on Signal and Information Processing, 317 (2013).
- [29] T. Ozaki, Ann. Inst. Stat. Math. **31**, 145 (1979).
- [30] Y. Ogata and K. Katsura, Geophys. J. Int. **113**, 727 (1993).
- [31] L. Paninski, Y. Ahmadian, D. G. Ferreira, S. Koyama, K. R. Rad, M. Vidne, J. Vogelstein, and W. Wu, J. Comput. Neurosci. **29**, 107 (2010).
- [32] T. Omi, Y. Ogata, Y. Hirata, and K. Aihara, Sci. Rep. **3**, 2218 (2013).
- [33] E. Bacry and J.-F. Muzy, Quant. Finance **14**, 1147 (2014).
- [34] V. Filimonov and D. Sornette, Quant. Finance **15**, 1293 (2015).
- [35] M. Lallouache and D. Challet, Quant. Finance **16**, 1 (2016).
- [36] T. Kumazawa, Y. Ogata, The Annals of Applied Statistics **8**, 1825 (2014).
- [37] C. M. Bishop, *Pattern Recognition and Machine Learning* (Springer, New York, 2006).
- [38] L. Tierney and J. B. Kadane, J. Am. Stat. Assoc. **81**, 82 (1986).
- [39] I. J. Good, *The Estimation Of Probabilities*, (MIT press, Cambridge, 1965).
- [40] H. Akaike, IEEE Transactions on Automatic Control **19**, 716 (1974).
- [41] G. Schwarz, The Annals of Statistics **6**, 461 (1978).
- [42] H. Akaike, Trabajos de estadística y de investigación operativa **31**, 143 (1980).

ACKNOWLEDGEMENTS

This work is supported by the Kozo Keikaku Engineering Inc. and CREST, JST.

APPENDIX A: CONSTRUCTING VARIABLE-WIDTH BASIS FUNCTIONS

A specific method to generate bump-shaped basis functions with variable width is described. Our method is schematically illustrated in Fig. 2. We first introduce a natural time coordinate t' , where the position t'_i of the i th event is equal to the index, $t'_i = i$ ($i = 1, 2, \dots, n$), and the start t'_0 and end t'_{n+1} of the observation interval are respectively 0 and $n + 1$ (Fig. 2b). We also place equally spaced knots with distance $w = (n + 1)/(m - 3)$ in the natural time coordinate t' , whose positions are $\xi_k = kw$ for integer k (vertical dotted lines in Fig. 2b). In this coordinate, we employ the m basis functions with fixed width as $F^j(t') = \tilde{f}((t' - \xi_{j-4})/w)$ ($j = 1, 2, \dots, m$), where $\tilde{f}(\cdot)$ is a cubic B-spline base in Fig. 2a. Next, we make a coordinate change from the natural time t' to the actual time t to obtain the basis functions $\{f^j(t)\}$

with variable width in the actual time coordinate t as $f^j(t) = F^j(\phi(t))$, where $\phi(t)$ is a monotonic function satisfying $\phi(t_i) = t'_i$ ($t_0 = S, t_{n+1} = T$), as shown in Fig. 2c. Although it is necessary to define a continuous function for $\phi(t)$ to obtain the appropriate coordinate change, we here simply approximate such a function as a piecewise constant function, that is, $\phi(t) = t'_i$ for $t_i \leq t < t_{i+1}$ ($i = 0, \dots, n$). This approximation gives the basis functions $\{f^j(t)\}_{j=1}^m$ that are constant during each inter-event period: $f^j(t) = f_i^j \equiv F^j(t'_i)$ for $t_i \leq t < t_{i+1}$ ($i = 0, 1, \dots, n$).

APPENDIX B: BAYESIAN ESTIMATION OF THE NON-STATIONARY MODEL

Our model is characterized by the parameters $\{\alpha, \beta, \mathbf{a}\}$, where $\mathbf{a} = (a_1, \dots, a_m)^T$, and the log likelihood function is given as

$$\log L(\mathbf{a}, \alpha, \beta | \mathbf{D}^{[S, T]}) = \sum_{i=1}^n \log \left[\mu_i + \sum_{k=1}^{i-1} \alpha \beta e^{-\beta(t_i - t_k)} \right] - \sum_{i=0}^n \mu_i (t_{i+1} - t_i) - \sum_{i=1}^n \alpha [1 - e^{-\beta(T - t_i)}], \quad (5)$$

where $\mu_i = \exp[\sum_{j=1}^m a_j f_i^j]$. In our case, the number of the parameters of \mathbf{a} is relatively large, the order of hundreds for some data analyzed in this study. In such a case, the maximum likelihood estimation gives a rough estimate of $\mu(t)$ due to overfitting and tends to be com-

putationally unstable. To robustly estimate such a large number of the parameters, we employ a Bayesian estimation approach. In the approach, we introduce a prior probability distribution of the parameters \mathbf{a} that restricts the flexibility of $\mu(t)$ to prevent overfitting, given as

$$P_{V, W, \mu_c}(\mathbf{a}) = \frac{1}{C} \exp \left[-\frac{V}{2} \sum_{i=1}^n \left(\frac{d}{dt'} \sum_{j=1}^m a_j F^j(t'_i) \right)^2 - \frac{W}{2} \left(\frac{\sum_{j=1}^m a_j}{m} - \log \mu_c \right)^2 \right], \quad (6)$$

where C is the normalizing constant, and V , W , and μ_c are additional parameters. The first term in the exponential penalizes the first derivative of $\log \mu(t') = \sum_{j=1}^m a_j F^j(t')$ in the natural time coordinate t' , and the parameter V controls the smoothness of $\mu(t)$ (also see Appendix C). The second term in the exponential restricts the average parameter value $\sum_{j=1}^m a_j/m$, which roughly corresponds to the baseline of $\log \mu(t)$, $\sum_{i=1}^n \log \mu(t_i)/n$. This term is introduced to make the prior normalizable; since the first term is invariant under the transformation $a_j \rightarrow a_j + c$ ($j = 1, \dots, m$) for constant c , which corresponds to the vertical shift $\log \mu(t) \rightarrow \log \mu(t) + c$ from the relation $\sum_{j=1}^m f_i^j = 1$, the prior only with the first term cannot be normalized. In this study, the parameter W is fixed to a very large value (e.g., 10^4) because the estimate of the model parameters $\{\alpha, \beta, \mathbf{a}\}$ remains nearly unchanged regardless of the value of W . In this

setting, we have a relation $\log \mu_c \simeq \sum_{i=1}^n \log \mu(t_i)/n$, so the parameter μ_c represents the baseline of $\mu(t)$. We also note that our non-stationary model reduces to the stationary process with $\mu(t) = \mu_c$ in the limit of $V \rightarrow \infty$ and $W \rightarrow \infty$.

In a Bayesian framework, we treat the parameters $\theta_h = \{\alpha, \beta, V, \mu_c\}$ as hyper-parameters, and estimate the hyper-parameters θ_h differently from the remaining parameters \mathbf{a} . We first consider a method to estimate the parameters \mathbf{a} under a given value of the hyper-parameters θ_h . From the Bayes' theorem [37], the posterior probability distribution of the parameters \mathbf{a} given the hyper-parameters θ_h is given by

$$P_{\theta_h}(\mathbf{a} | \mathbf{D}^{[S, T]}) \propto L(\mathbf{a}, \alpha, \beta | \mathbf{D}^{[S, T]}) P_{V, \mu_c}(\mathbf{a}). \quad (7)$$

The maximum a posteriori (MAP) estimate \mathbf{a}^* is obtained by maximizing the logarithm of the posterior.

Then we consider to find the optimal estimate of the hyper-parameters θ_h . The goodness-of-fit to the data of the model with the hyper-parameters θ_h is characterized by the marginal likelihood function, also known as the

evidence, given as

$$ML(\theta_h|D^{[S,T]}) = \int L(\mathbf{a}, \alpha, \beta|\mathbf{D}^{[S,T]}) P_{V,\mu_c}(\mathbf{a}) d\mathbf{a}. \quad (8)$$

We approximately calculate the marginal likelihood function by using Laplace's method [38]; the logarithm of the integrand is expanded to the second order of \mathbf{a} around its peak. In our case, the peak is located at $\mathbf{a} = \mathbf{a}^*$, which is the MAP estimate. We then obtain

$$\log ML(\theta_h|D^{[S,T]}) \simeq \frac{m}{2} \log 2\pi - \frac{1}{2} \log \det(H) + \log L(\mathbf{a}^*, \alpha, \beta|\mathbf{D}^{[S,T]}) + \log P_{V,\mu_c}(\mathbf{a}^*), \quad (9)$$

where H represents the Hessian matrix of the minus of the logarithm of the integrand at $\mathbf{a} = \mathbf{a}^*$. The estimate θ_h^* of the hyper-parameters is obtained by maximizing the logarithm of the marginal likelihood function [39]. The optimal estimate of the parameter set $\{\mathbf{a}^*, \theta_h^*\}$ is finally obtained as the optimal estimate of the hyper parameters θ_h^* and the MAP estimate \mathbf{a}^* under the optimal hyper-parameters θ_h^* .

APPENDIX C: MODEL SELECTION

In the text, we compare the goodness-of-fit to the data between the stationary and non-stationary Hawkes models. The log-likelihood is not a good measure of the goodness-of-fit in comparing models with different levels of complexity, because the log-likelihood of a complex model overestimates the goodness-of-fit due to overfitting. Therefore it is a standard task to add a penalty on the log likelihood depending on the model complex-

ity [40, 41]. For the stationary Hawkes model, we use a score $S_S = \arg \max_{\theta} \log L(\theta|D) - 3$ to measure the goodness-of-fit based on the Akaike information criterion [40], where 3 in the score represents the number of parameters in $\theta = \{\alpha, \beta, \mu_c\}$. For the non-stationary Hawkes model estimated in the Bayesian method, we use a score $S_{NS} = \arg \max_{\theta_h} \log ML(\theta_h|D) - 4$ based on the Akaike Bayesian information criterion [42], where $ML(\theta_h|D)$ is the marginal likelihood in Eq. (9) and 4 in the score corresponds to the number of the free hyper-parameters in $\theta_h = \{\alpha, \beta, \mu_c, V\}$. It is noted that the penalty on the model complexity coming from the parameters \mathbf{a} that account for the time variation of $\mu(t)$ is naturally included in the log marginal likelihood. We can rewrite Eq. (9) as $\log ML = \log L - (Penalty)$. The complexity of the temporal variation in $\mu(t)$ is controlled by the hyper-parameter V ; the estimated $\mu(t)$ is almost constant for a large value of V , and the estimated $\mu(t)$ much varies in time for a small value of V . The penalty term is almost 0 for the large value of V (low complexity), and scales with $m \log(1/V)$ for the small value of V (high complexity).